

Realization and characterization of a 2-photon 4-qubit linear cluster state

Giuseppe Vallone^{1,*}, Enrico Pomarico^{1,*}, Paolo Mataloni^{1,*}, Francesco De Martini^{1,*}, Vincenzo Berardi²

¹Dipartimento di Fisica dell'Università "La Sapienza" and Consorzio Nazionale

Interuniversitario per le Scienze Fisiche della Materia, Roma, 00185 Italy

²Dipartimento Interateneo di Fisica, Università e Politecnico di Bari and Consorzio Nazionale Interuniversitario per le Scienze Fisiche della Materia, Bari, 70126 Italy

We report on the experimental realization of a 4-qubit linear cluster state via two photons entangled both in polarization and linear momentum. This state was investigated by performing tomographic measurements and by evaluating an entanglement witness. By use of this state we carried out a novel nonlocality proof, the so-called "stronger two observer all versus nothing" test of quantum nonlocality.

PACS numbers: 03.67.Mn, 03.65.Ud, 42.50.Xa

Multipartite graph states and, in particular, cluster states, have been recently introduced by Briegel and Raussendorf as a fundamental resource aimed at the linear optics one way quantum computation [1, 2], and at the realization of important quantum information tasks, such as quantum error correction and quantum communication protocols [3, 4]. Recently, the experimental feasibility of one way quantum computation by four photon cluster states was demonstrated [5, 6]. Besides the applications to quantum computation, cluster states are powerful tools for performing nonlocality tests [7, 8]. It is well known that the adoption of an increasing number of internal qubits, i.e. in a higher dimensional Hilbert space, leads to a stronger violation of local realism [9]. Recently, a test demonstrating that nonlocality grows with the number of internal degrees of freedom of the system, was indeed successfully carried out by taking advantage of the peculiar properties of a 2-photon hyperentangled state [10]. It is worth noting that, at variance with the cluster states, hyperentangled, or double entangled states, are bi-separable and do not represent genuine four-qubit entangled states.

In this letter we report the experimental realization of a high fidelity 2-photon 4-qubit linear cluster state by a linear optical technique consisting of the entanglement of the polarization (π) and momentum (\mathbf{k}) degrees of freedom of one of the two photons belonging to an hyperentangled state. The cluster state was analyzed by quantum tomographic measurements and by an entanglement witness method [8, 11]. By using this state, we performed a novel "All-Versus-Nothing" (AVN) test of nonlocality recently proposed by Cabello [12].

As said, the starting point for the cluster state generation was the hyperentangled state $|\Xi\rangle = |\Phi^-\rangle \otimes |\psi^+\rangle$, where $|\Phi^-\rangle = \frac{1}{\sqrt{2}}(|H\rangle_A|H\rangle_B - |V\rangle_A|V\rangle_B)$ and $|\psi^+\rangle = \frac{1}{\sqrt{2}}(|r\rangle_A|\ell\rangle_B + |\ell\rangle_A|r\rangle_B)$. In the above equations H, V refer to the horizontal (H) and vertical (V) polarizations and ℓ, r refer to the left (ℓ) or right (r) paths of the photon A (Alice) or B (Bob) (see Fig. 1). The state $|\Xi\rangle$ is realized by a Spontaneous Parametric Down Conversion

(SPDC) method already described in details in other papers [13, 14]. A thin type I β -barium-borate BBO crystal slab operating under the double (back and forth) excitation of a cw Ar^+ laser ($\lambda_p = 364$ nm) generated the π -entangled state $|\Phi^-\rangle$, obtained by the superposition of two perpendicularly polarized SPDC cones emerging from the crystal at the degenerate wavelength $\lambda = 728$ nm. The \mathbf{k} -entangled state $|\psi^+\rangle$ was realized by selecting two pairs of correlated \mathbf{k} -modes, $r_A-\ell_B$ and ℓ_A-r_B , belonging to the conical emission of the crystal. Because of the "phase-preserving" character of the SPDC process, the relative phase between the two pair emissions was set to the value $\phi = 0$. By adoption of hyperentangled states several AVN tests of quantum nonlocality were recently proposed [15] and carried out [16].

In the present experiment the 2-photon 4-qubit linear

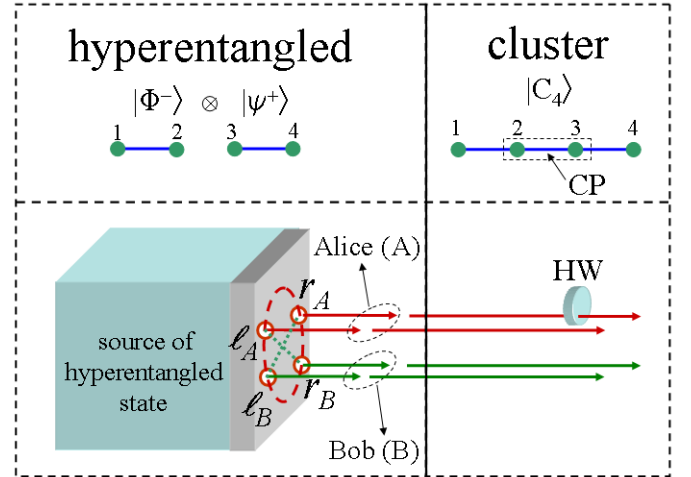


FIG. 1: Generation of the linear cluster state by a source of polarization-momentum hyperentangled 2-photon state. The state $|\Xi\rangle = |\Phi^-\rangle \otimes |\psi^+\rangle$ corresponds to two separate 2-qubit clusters. The HW acts as a Controlled-Phase (CP) thus generating the 4-qubit linear cluster $|C_4\rangle$.

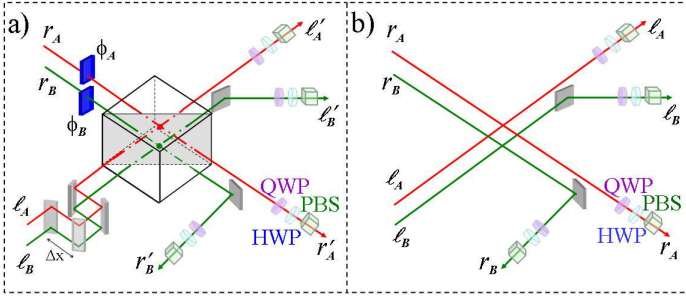


FIG. 2: Interferometer and measurement apparatus. a) The mode pairs $r_A\text{-}l_B$ and $l_A\text{-}r_B$ are matched on the BS. The phase shifters ϕ_A and ϕ_B (thin glass plates) are used for the measurement of momentum observables. The polarization analyzers on each of BS output modes are shown (QWP/HWP=Quarter/Half-Wave Plate, PBS=Polarized Beam Splitter). b) Same configuration as in a) with BS and glasses removed.

cluster state

$$\begin{aligned}
 |C_4\rangle &= \frac{1}{2} (|Hr\rangle_A |Hl\rangle_B + |Vr\rangle_A |Vl\rangle_B \\
 &\quad + |Hl\rangle_A |Hr\rangle_B - |Vl\rangle_A |Vr\rangle_B) \quad (1) \\
 &= \frac{1}{\sqrt{2}} (|\Phi^+\rangle |r\rangle_A |l\rangle_B + |\Phi^-\rangle |l\rangle_A |r\rangle_B),
 \end{aligned}$$

where $|\Phi^+\rangle = \frac{1}{\sqrt{2}}(|H\rangle_A |H\rangle_B + |V\rangle_A |V\rangle_B)$, was created by inserting in the r_A (right-Alice) mode a zero order half wave plate (HW) with the optical axis oriented along the vertical direction (see Fig. 1). The HW left the state $|\Phi^-\rangle |l\rangle_A |r\rangle_B$ unchanged, while the transformation $|\Phi^-\rangle |r\rangle_A |l\rangle_B$ into $|\Phi^+\rangle |r\rangle_A |l\rangle_B$ also transformed $|\Xi\rangle$ into $|C_4\rangle$.

Under the correspondence $|H\rangle_{A,B} \leftrightarrow |0\rangle_{2,1}$, $|V\rangle_{A,B} \leftrightarrow |1\rangle_{2,1}$ and $|l\rangle_{A,B} \leftrightarrow |0\rangle_{3,4}$, $|r\rangle_{A,B} \leftrightarrow |1\rangle_{3,4}$, the state (1) is equivalent to the cluster state [19] expressed in the logical basis $|0\rangle$ and $|1\rangle$

$$\begin{aligned}
 |\tilde{C}_4\rangle &= \frac{1}{2} (|0\rangle_1 |0\rangle_2 |1\rangle_3 |0\rangle_4 + |1\rangle_1 |1\rangle_2 |1\rangle_3 |0\rangle_4 \\
 &\quad + |0\rangle_1 |0\rangle_2 |0\rangle_3 |1\rangle_4 - |1\rangle_1 |1\rangle_2 |0\rangle_3 |1\rangle_4). \quad (2)
 \end{aligned}$$

It is worth stressing that the insertion of HW represents a ‘‘local’’ operation in the sense that it acts on photon A only, while it is ‘‘nonlocal’’ for the two qubits associated to photon A itself. Indeed, the HW operates as a Controlled Phase (CP) between the target qubit 2 and the control qubit 3 (i.e. the polarization and the momentum degree of freedom of photon A), thus entangling the four qubits together. Moreover this operation does not require any kind of post-selection.

Let’s consider the measurement setup shown in Fig. 2a). The mode pairs $r_A\text{-}l_B$ and $l_A\text{-}r_B$ are there spatially and temporally superimposed by means of a 50%

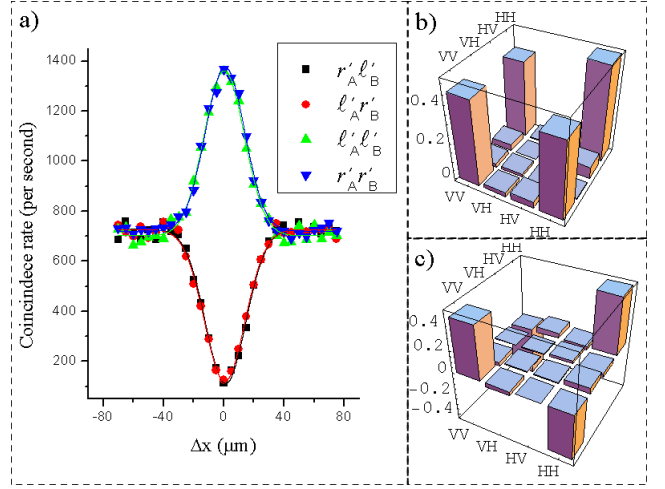


FIG. 3: State characterization. a) Coincidence rates versus path delay Δx showing the interference pattern between the two pairs $r_A\text{-}l_B$ and $l_A\text{-}r_B$. The dip(peak) FWHM and the coherence time ($\sim 150\text{fsec}$) of the photons are determined by the bandwidth (6nm) of the interference filter used. b) and c) Tomographic reconstructions (real parts) of the polarization states corresponding to $|\Phi^+\rangle$ and $|\Phi^-\rangle$ respectively. The imaginary components are negligible. Typical uncertainties are 0.006 for the higher terms ($|\langle HH \rangle|$, $|\langle HH \rangle|$, $|\langle HH \rangle|$, $|\langle VV \rangle|$, $|\langle VV \rangle|$ and $|\langle VV \rangle|$) and 0.003 for the other terms.

beam splitter (BS). The optical path delay Δx can be simultaneously changed for both l_A and l_B modes by using a trombone mirror assembly. The null value delay ($\Delta x = 0$) corresponds to the exact superposition on the BS between $r_A\text{-}l_B$ and $l_A\text{-}r_B$, i.e. when the right (r) and left (l) optical paths are equal [13]. The two thin glass plates inserted on the right modes (ϕ_A and ϕ_B in Fig. 2a)) and the BS transform the input states in the following way: $\frac{1}{\sqrt{2}}(|l\rangle_i + e^{-i\phi_i}|r\rangle_i) \rightarrow |l'\rangle_i$, $\frac{1}{\sqrt{2}}(|l\rangle_i - e^{-i\phi_i}|r\rangle_i) \rightarrow |r'\rangle_i$ with $i = A, B$. Note that these are single photon transformations: in fact the single BS showed in Fig. 2a) is equivalent to two BS’s, one for each (A or B) particle. The reason why we used the single BS apparatus resides on its higher phase stability.

The photons associated with the BS output modes l'_A , r'_B , l'_B and r'_A are analyzed each by a quarter-wave plate (QWP), half-wave plate (HWP), a polarizing beam splitter (PBS) and detected by single photon avalanche detectors. Two thin glass plates on modes r_A and r_B are properly set for measuring momentum observables. The analysis setup shown in Fig. 2b) is obtained from Fig. 2a) by removing the interferometric apparatus and allows the measurement of several relevancy observables that will be introduced later in the paper.

We characterized the state (1) by measuring the interference between the mode pairs $r_A\text{-}l_B$ and $l_A\text{-}r_B$ as a function of the delay Δx . The dip-peak graph (88% average visibility) for H polarized photons, corresponding to the \mathbf{k} -entangled state $|\psi^+\rangle$, is shown in Fig. 3a).

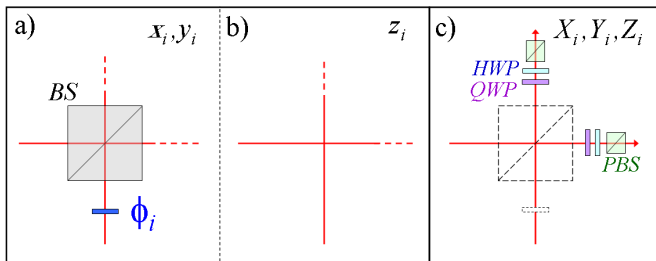


FIG. 4: Measurement setup for momentum (a,b)) and polarization (c)) observables for photon i ($i=A, B$). By the a) setup we measure x_i ($\phi_i = 0$) and y_i ($\phi_i = \frac{\pi}{2}$), while the b) setup is used for measuring z_i . By the c) setup we measure X_i ($\theta_Q = \frac{\pi}{4}$; $\theta_H = \frac{1}{8}\pi, \frac{3}{8}\pi$), Y_i ($\theta_Q = 0$; $\theta_H = \frac{1}{8}\pi, \frac{3}{8}\pi$) and Z_i ($\theta_Q = 0$; $\theta_H = 0, \frac{\pi}{4}$), where $\theta_{H(Q)}$ is the angle between the $HWP(QWP)$ optical axis and the vertical direction. The polarization analysis is performed contextually to x_i, y_i (i.e. with BS and glass) or z_i (without BS and glass), as shown by the dotted lines for BS and glass in c).

Similar results are obtained for V polarized photons with dips and peaks flipped [20]. By removing the BS (Fig. 2b)), we performed a quantum tomographic analysis on the mode sets $r_A\text{-}\ell_B$ and $\ell_A\text{-}r_B$, corresponding to the π -entangled states $|\Phi^+\rangle$ (Fig. 3b)) and $|\Phi^-\rangle$ (Fig. 3c)) respectively. The tomographic reconstructions were obtained by the ‘‘Maximum Likelihood Estimation’’ method described in [17]. The corresponding fidelities are $F_{|\Phi^+\rangle} = 0.9068 \pm 0.0035$ and $F_{|\Phi^-\rangle} = 0.9131 \pm 0.0032$. Note that the path interference measurement shown in Fig. 3a) demonstrates the quantum superposition between the two states $|\Phi^+\rangle|r\rangle_A|\ell\rangle_B$ and $|\Phi^-\rangle|\ell\rangle_A|r\rangle_B$ of Fig. 3b) and 3c), leading to the linear cluster state (1).

The genuine multipartite 4-qubit entanglement was verified by measuring the entanglement witness [11]

$$\mathcal{W} = \frac{1}{2} [4\mathbb{1} - Z_A Z_B - Z_A x_A x_B + X_A z_A X_B + z_A z_B - x_A Z_B x_B - X_A X_B z_B] \quad (3)$$

where upper cases refer to polarization operators

$$\begin{aligned} Z_i &= |H\rangle_i \langle H| - |V\rangle_i \langle V| \\ Y_i &= i|V\rangle_i \langle H| - i|H\rangle_i \langle V| \\ X_i &= |H\rangle_i \langle V| + |V\rangle_i \langle H| \end{aligned} \quad i = A, B \quad (4)$$

and lower cases refer to momentum operators

$$\begin{aligned} z_i &= |\ell\rangle_i \langle \ell| - |r\rangle_i \langle r| \\ y_i &= i|r\rangle_i \langle \ell| - i|\ell\rangle_i \langle r| \\ x_i &= |\ell\rangle_i \langle r| + |r\rangle_i \langle \ell| \end{aligned} \quad i = A, B \quad (5)$$

The experimental setups for measuring the polarization (4) and momentum (5) observables for either Alice or Bob photon are shown in Fig. 4. Note that the eigenvectors of x_i and y_i can be written in the form $\frac{1}{\sqrt{2}}(|\ell\rangle_i \pm e^{-i\phi_i}|r\rangle_i)$.

Observable	Value	\mathcal{W}	S	C
$Z_A Z_B$	$+0.9283 \pm 0.0032$	✓		
$Z_A x_A x_B$	$+0.8194 \pm 0.0049$	✓		
$X_A z_A X_B$	-0.9074 ± 0.0037	✓		✓
$z_A z_B$	-0.9951 ± 0.0009	✓		✓
$x_A Z_B x_B$	$+0.8110 \pm 0.0050$	✓		✓
$Z_A y_A y_B$	$+0.8071 \pm 0.0050$			✓
$Y_A z_A Y_B$	$+0.8948 \pm 0.0040$			✓
$X_A X_B z_B$	$+0.9074 \pm 0.0037$	✓	✓	✓
$Y_A Y_B z_B$	-0.8936 ± 0.0041		✓	✓
$X_A x_A Y_B y_B$	$+0.8177 \pm 0.0055$		✓	
$Y_A x_A X_B y_B$	$+0.7959 \pm 0.0055$		✓	

TABLE I: Experimental values of the observables used for measuring the entanglement witness \mathcal{W} and the expectation value of S on the cluster state $|C_4\rangle$. The third column (C) refers to the control measurements needed to verify that $X_A, Y_A, x_A, X_B, Y_B, y_B$ and z_B can be considered as elements of reality. Each experimental value corresponds to a measure lasting an average time of 10 sec. In the experimental errors we considered the poissonian statistic and the uncertainties due to the manual setting of the polarization analysis wave plates.

Those states can be discriminated, as previously explained, by the glass plates and the BS.

The expectation value of \mathcal{W} is positive for any separable state (for instance it is equal to 1 for the hyper-entangled state $|\Xi\rangle$), whereas its negative value detects 4-party entanglement close to the cluster state (1). A perfect cluster state gives -1 as expectation value.

The experimental values of the observables of eq. (3) are shown in Table I. The non perfect correlations were due to the impurity of the states $|\Phi^+\rangle$ and $|\Phi^-\rangle$, as well as to imperfections in the polarization and momentum analysis devices. The resulting experimental value of \mathcal{W} is

$$\text{Tr}[\mathcal{W}\rho_{exp}] = -0.6843 \pm 0.0094, \quad (6)$$

thus demonstrating the genuine multipartite entanglement of our cluster state, whose ρ_{exp} represents the experimental density matrix.

From the projector-based entanglement witness [11] $\widetilde{\mathcal{W}} = \frac{1}{2} - |C_4\rangle\langle C_4|$, we could obtain information about the fidelity $F_{|C_4\rangle}$ of the state through the equation $F_{|C_4\rangle} = \frac{1}{2} - \text{Tr}[\widetilde{\mathcal{W}}\rho_{exp}]$. As shown in [11], the following relation holds between \mathcal{W} and $\widetilde{\mathcal{W}}$: $\mathcal{W} - 2\widetilde{\mathcal{W}} \geq 0$. Hence the lower bound of the experimental fidelity $F_{|C_4\rangle}$ is:

$$F_{|C_4\rangle} \geq \frac{1}{2} - \frac{1}{2}\text{Tr}[\mathcal{W}\rho_{exp}] \geq 0.84, \quad (7)$$

giving a further evidence of the cluster generation.

Finally, we tested the nonlocal character of our cluster state by using the ‘‘stronger two observer AVN’’ proof of

local realism, recently introduced in [12]. It is based on the following eigenvalue equations:

$$X_A z_A X_B |C_4\rangle = -|C_4\rangle \quad (8a)$$

$$z_A z_B |C_4\rangle = -|C_4\rangle \quad (8b)$$

$$x_A Z_B x_B |C_4\rangle = +|C_4\rangle \quad (8c)$$

$$Z_A y_A y_B |C_4\rangle = +|C_4\rangle \quad (8d)$$

$$Y_A z_A Y_B |C_4\rangle = +|C_4\rangle \quad (8e)$$

$$X_A X_B z_B |C_4\rangle = +|C_4\rangle \quad (8f)$$

$$Y_A Y_B z_B |C_4\rangle = -|C_4\rangle \quad (8g)$$

$$X_A x_A Y_B y_B |C_4\rangle = +|C_4\rangle \quad (8h)$$

$$Y_A x_A X_B y_B |C_4\rangle = +|C_4\rangle \quad (8i)$$

The first seven equalities demonstrate that the local observables $X_A, Y_A, x_A, X_B, Y_B, y_B$ and z_B are elements of reality in the EPR sense [18]. The last four equalities are used in the AVN proof through the following quantum mechanical expectation value of the cluster state (1):

$$\langle S \rangle = \langle C_4 | X_A X_B z_B - Y_A Y_B z_B + X_A x_A Y_A y_B + Y_A x_A X_A y_B | C_4 \rangle = 4 \quad (9)$$

In any local realistic theory based on the previously defined elements of reality, the upper bound of the expected value for eq. (9) is 2.

From the experimental values given in Table I we obtain

$$\text{Tr}[S\rho_{exp}] = 3.4145 \pm 0.0095, \quad (10)$$

which violates the classical bound by 148 standard deviations. Note that this result provides another enhanced discrepancies between the quantum versus classical predictions (4 versus 2) with respect to the standard CHSH inequality ($2\sqrt{2}$ versus 2) [10].

In summary, in this letter we have presented the experimental realization of a high fidelity linear cluster state consisting of four entangled qubits by adoption of 2-photon polarization-momentum hyperentanglement within a linear optical method. The cluster state was generated by applying a CP gate between the polarization and momentum qubits of one photon of the hyperentangled state. The genuine entangled character of the cluster state was experimentally demonstrated. Its non-local behaviour was also tested by a novel AVN quantum mechanical test proposed for 2-photon linear cluster state.

Other kinds of cluster states can be easily produced by the same technique presented here. Apart for the relevance of these states for fundamental physics, two photon cluster states may be good candidates to realize important quantum information tasks because of their high purity and the relatively high generation rate. Whether or not these states may also represent a useful resource for linear optics quantum computation is as yet unclear. In

fact our method could be used in probabilistic quantum computation with the advantage of high counting rates. Moreover, two $|C_4\rangle$ states generated by the same laser source could be linked together by a suitable CP gate to form an 8-qubit linear cluster state.

Thanks are due to Adán Cabello for useful discussions and Marco Barbieri for his contribution in planning the experiment. This work was supported by the FIRB 2001 (Realization of Quantum Teleportation and Quantum Cloning by the Optical Parametric Squeezing Process) and PRIN 2005 (New perspectives in entanglement and hyper-entanglement generation and manipulation) of MIUR (Italy).

*Electronic address: <http://quantumoptics.phys.uniroma1.it/>

-
- [1] H. J. Briegel and R. Raussendorf, Phys. Rev. Lett. **86**, 910 (2001).
 - [2] H. J. Briegel and R. Raussendorf, Phys. Rev. Lett. **86**, 5188 (2001).
 - [3] D. Schlingemann, R.F. Werner, Phys. Rev. A, **65**, 012308 (2002).
 - [4] R. Cleve, D. Gottesmann, H.-K. Lo, Phys. Rev. Lett. **83**, 648 (1999); M. Hillery et al., Phys. Rev. A, **58**, 1829 (1999).
 - [5] P. Walther et al., Nature **434**, 169 (2005).
 - [6] M.S. Tame et al. quant-ph/0611186.
 - [7] P. Walther et al., Phys. Rev. Lett. **95**, 020403 (2005).
 - [8] Kiesel et al., Phys. Rev. Lett. **95**, 210502 (2005).
 - [9] N. D. Mermin, Phys. Rev. Lett. **65**, 1838 (1990); A. Cabello, *ibid.* **97**, 140406, (2006).
 - [10] M. Barbieri, F. De Martini, P. Mataloni, G. Vallone, A. Cabello, Phys. Rev. Lett. **97**, 140407 (2006).
 - [11] G. Tóth, O. Gühne, Phys. Rev. A **72**, 022340 (2005).
 - [12] A. Cabello, Phys. Rev. Lett. **95**, 210401 (2005).
 - [13] M. Barbieri, C. Cinelli, F. De Martini, P. Mataloni, Phys. Rev. A **72**, 052110 (2005).
 - [14] C. Cinelli, G. Di Nepi, F. De Martini, M. Barbieri, P. Mataloni, Phys. Rev. A **70**, 022321 (2004).
 - [15] Z.B. Chen, J.W. Pan, Y.D. Zhang, Č. Brukner and A. Zeilinger, Phys. Rev. Lett. **90**, 160408 (2003); A. Cabello, *ibid.* **87**, 010403 (2001).
 - [16] T. Yang, Q. Zhang, J. Zhang, J. Yin, Z. Zhao, M. Zukowski, Z.B. Chen and J.W. Pan, Phys. Rev. Lett. **95**, 240406 (2005); C. Cinelli, M. Barbieri, R. Perris, P. Mataloni, F. De Martini, *ibid.* **95**, 240405 (2005);
 - [17] D.F.V. James, P.G. Kwiat, W.J. Munro and A.G. White, Phys. Rev. A **64**, 052312 (2001).
 - [18] A. Einstein, B. Podolsky and N. Rosen, Phys. Rev. **47**, 777 (1935)
 - [19] The state (2) is equivalent to the linear cluster state $|\phi_4\rangle = \frac{1}{2}(|0000\rangle + |1100\rangle + |0011\rangle - |1111\rangle)$, generated in [8], up to a σ_x operation on the third qubit.
 - [20] The cluster state (1) can be also written as $|\Xi\rangle = \frac{1}{\sqrt{2}}(|H\rangle_A |H\rangle_B |\psi^+\rangle + |V\rangle_A |V\rangle_B |\psi^-\rangle)$ where $|\psi^\pm\rangle = \frac{1}{\sqrt{2}}(|r\rangle_A |\ell\rangle_B - |\ell\rangle_A |r\rangle_B)$, then dips and peaks are flipped for V photons.